Novel artificial tricalcium phosphate and magnesium composite graft facilitates angiogenesis in bone healing

Yuan-Hsin Tsai, Chun-Chieh Tseng, Yun-Chan Lin, Howida M. Nail, Kuan-Yu Chiu, Yen-Hao Chang, Ming-Wei Chang, Feng-Huei Lin, Hui-Min David Wang

PII: S2319-4170(24)00053-2

DOI: https://doi.org/10.1016/j.bj.2024.100750

Reference: BJ 100750

To appear in: *Biomedical Journal*

Received Date: 31 March 2023

Revised Date: 22 March 2024

Accepted Date: 30 May 2024

Please cite this article as: Tsai Y-H, Tseng C-C, Lin Y-C, Nail HM, Chiu K-Y, Chang Y-H, Chang M-W, Lin F-H, Wang H-MD, Novel artificial tricalcium phosphate and magnesium composite graft facilitates angiogenesis in bone healing, *Biomedical Journal*, https://doi.org/10.1016/j.bj.2024.100750.

Novel artificial tricalcium phosphate and magnesium composite graft facilitates angiogenesis in bone healing

Yuan-Hsin Tsai [1,2], Chun-Chieh Tseng [3,4], Yun-Chan Lin [5], Howida M. Nail [6], Kuan-Yu Chiu [3,4], Yen-Hao Chang [3,4], Ming-Wei Chang [7], Feng-Huei Lin [8,9,10*], and Hui-Min David Wang [6,11,12*]

Affiliations:

[1] Ph.D. Program in Tissue Engineering and Regenerative Medicine, National Chung Hsing University, Taichung 402, Taiwan, Republic of China

[2] Department of Orthopedic Surgery, Show-Chwan Memorial Hospital, Changhua 500, Taiwan, Republic of China

[3] Metal Industries Research & Development Centre, 1001 Kaonan Highway, Nanzi Dist., Kaohsiung 811, Taiwan, Republic of China

[4] Combination Medical Device Technology Division, Medical Devices R&D Service Department, Metal Industries Research & Development Centre, Kaohsiung 802, Taiwan, Republic of China

[5] Department of Food Science and Biotechnology, National Chung Hsing University, Taichung 402, Taiwan, Republic of China

[6] Graduate Institute of Biomedical Engineering, National Chung Hsing University, Taichung 402, Taiwan, Republic of China

[7] Nanotechnology and Integrated Bioengineering Centre, University of Ulster, Belfast, BT15 1AB, Northern Ireland, UK

[8] Ph.D. Program in Tissue Engineering and Regenerative Medicine, National Chung Hsing University, Taichung 402, Taiwan, Republic of China

[9] Institute of Biomedical Engineering, College of Medicine and College of Engineering, National Taiwan University, Taipei, Taiwan, Republic of China

[10] Institute of Biomedical Engineering and Nano-medicine, National Health Research Institutes, Zhunan, Miaoli 350, Taiwan, Republic of China

[11] Graduate Institute of Medicine, College of Medicine, Kaohsiung Medical University, Kaohsiung 807, Taiwan, Republic of China

[12] Department of Medical Laboratory Science and Biotechnology, China Medical University, Taichung City 404, Taiwan, Republic of China

Corresponding Authors*

Feng-Huei Lin, Ph.D

Professor, Institute of Biomedical Engineering, College of Medicine and College of Engineering, National Taiwan University, No. 1, Sec. 4, Roosevelt Rd, Taipei 10617, Taiwan, Republic of China

Distinguished Investigator and Director, Division of Biomedical Engineering and Nanomedicine Research, National Health Research Institutes, No. 35, Keyan Road, Zhunan, Miaoli County 35053, Taiwan, Republic of China

E-mail: double@ntu.edu.tw

Telephone: +886-2-2732-7474

Hui-Min David Wang, Ph.D. (H.-M. W.)

Professor, Graduate Institute of Biomedical Engineering, National Chung Hsing University, Taichung 402, Taiwan, Republic of China

Address: No.145, Xingda Rd., South Dist., Taichung City 402, Taiwan, Republic of China

Mobil: 886-935753718

TEL: 886-4-2284-0733#651

Fax: 886-4-22852242

E-mail: davidw@dragon.nchu.edu.tw

ORCID: https://orcid.org/0000-0002-4692-4917

Website: https://sites.google.com/view/davidbiocosme/home?authuser=0

Abstract

Background: Bone grafting is the standard treatment for critical bone defects, but autologous grafts have limitations like donor site morbidity and limited availability, while commercial artificial grafts may have poor integration with surrounding bone tissue, leading to delayed healing. Magnesium deficiency negatively impacts angiogenesis and bone repair. Therefore, incorporating magnesium into a synthetic biomaterial could provide an excellent bone substitute. This study aims to evaluate the morphological, mechanical, and biological properties of a calcium phosphate cement (CPC) sponge composed of tetracalcium phosphate (TTCP) and monocalcium phosphate monohydrate (MCPM), which could serve as an excellent bone substitute by incorporating magnesium.

Methods: This study aims to develop biomedical materials composed mainly of TTCP and MCPM powder, magnesium powder, and collagen. The materials were prepared using a wet-stirred mill and freeze-dryer methods. The particle size, composition, and microstructure of the materials were investigated. Finally, the biological properties of these materials, including 3-(4,5-dimethylthiazol-2-yl)-2,5- diphenyltetrazolium bromide (MTT) assay for biocompatibility, effects on bone cell differentiation by alkaline phosphatase (ALP) activity assay and tartrate-resistant acid phosphatase

(TRAP) activity assay, and endothelial cell tube formation assay for angiogenesis, were evaluated as well.

Results: The data showed that the sub-micron CPC powder, composed of TTCP/MCPM in a 3.5:1 ratio, had a setting time shorter than 15 minutes and a compressive strength of 4.39±0.96 MPa. This reveals that the sub-micron CPC powder had an adequate setting time and mechanical strength. We found that the sub-micron CPC sponge containing magnesium had better biocompatibility, including increased proliferation and osteogenic induction effects without cytotoxicity. The CPC sponge containing magnesium also promoted angiogenesis.

Conclusion: In summary, we introduced a novel CPC sponge, which had a similar property to human bone promoted the biological functions of bone cells, and could serve as a promising material used in bone regeneration for critical bone defects.

Keywords: Critical bone defect, Magnesium, Tricalcium Phosphate, Bone graft

Introduction

Bone is a complex organ that has the ability for regeneration during development, or remodeling in adult life, as well as fracture healing [1]. Bone defects are deficiencies of bone where they should normally occur. The reasons for bone defects include trauma, tumor, or infection (osteomyelitis) [2]. Bone defects commonly influence patients' life quality, and the related medical treatment and costs are increasing. Currently, a major research topic in bones is bone defect regeneration [3]. However, in some cases, bone regeneration requires a large quantity for bone reconstruction with extreme bone defects, such as trauma, infection, tumor resection, and skeletal abnormalities. Moreover, a bone defect greater than 5 cm, known as a large-scale bone defect, impairs bone regeneration and leads to poor bone healing [4].

The standard therapeutic regimen to enhance bone regeneration for defects smaller than 5 cm is direct bone grafting [5, 6], which includes the use of various bone-grafting methods, including autografts, allografts, and bone-graft substitutes that enhance bone regeneration [7]. Vascularized bone grafts, harvesting cortico-cancellous graft with a vascular pedicle, offer predictable incorporation for defects larger than 12 cm [8, 9]. Defects larger than 12 cm are best treated using the distraction osteogenesis technique [10] and induced membrane technique [11]. The induced membrane technique, also

named the Masquelet Technique, is the use of a transient cement spacer followed by a staged large amount of bone grafting. To date, an autograft is still used as the most favorable standard because the requirements for bone regeneration are satisfied, for example, osteoinduction, osteoconduction, and osteogenesis [6, 12, 13]. However, the limitation is the number of donor and donor site complications. In the USA, the allograft is the second most popular bone graft, making up approximately 30% of all bone grafts [14]. Nevertheless, compared with the autograft, poor healing has been identified, and some adverse events such as disease transmission and other infectious pathogens have been reported [15, 16].

In the past decades, bone-graft substitutes were introduced to solve these concerns, with promising results. The bone substitutes should be architecturally like real bone and have the ability to afford a scaffold for osteoconductivity and growth factors for osteoinductivity. These materials are composed of synthetic or natural biomaterial scaffolds that promote the migration, proliferation, and differentiation of cells required for bone regeneration. For example, collagen, hydroxyapatite (HA), β-tricalcium phosphate (β-TCP), calcium-phosphate cement types, and glass ceramics are all commonly used in clinical settings, either alone or in combination. Moreover, the growth factors, including recombinant human bone morphological proteins (BMP-2

and BMP-7), necessary for bone regeneration, are provided in the scaffolds [17]. Since the osteoinductive properties of BMPs promote fracture healing, the clinical applications of BMPs are still limited due to the extremely high dosage, adverse effects, and cost [18].

The bone is a rich mineral reservoir, storing about 60% of the body's magnesium. Magnesium has a role in bone formation by inducing osteoblast proliferation and increasing the solubility of minerals. To maintain extracellular physiological cation concentrations at homeostasis, magnesium is released from the storage into the bloodstream [19]. In addition to its role in the crystal structure, magnesium is important for different physiological functions among living cells, such as those residents in bone. Based on this conception, magnesium homeostasis is critical for bone health. Previous reports have found that magnesium deficiency could induce osteoporosis in the rat and an increased formation of osteoclasts [20]. Moreover, magnesium was found to enhance osteogenesis in mesenchymal stem cells by the Notch signal pathway [21]. The magnesium-containing scaffolds have been used to enhance bone regeneration in vivo [22-25]. In this study, wet comminution in stirred media mills was used to produce sub-micron material of calcium phosphate bone cement sponge (CPC sponge) from tetracalcium phosphate/ monocalcium phosphate monohydrate (TTCP/MCPM)-based

144 calcium phosphate types of cement, followed by magnesium providing and collagen
145 covering. This study aims to analyze the *in vitro* morphological, mechanical, as well as
146 biological properties of the TTCP/MCPM nanoparticles.

147

148 Materials and methods

149 *Preparation of sub-micron TTCP/MCPM*

150 TTCP and MCPM were synthesized from calcium hydrogen phosphate and calcium
151 carbonate. TTCP was obtained by mixing calcium hydrogen phosphate and calcium
152 carbonate in a 1:1 molar ratio, followed by a high-temperature reaction at 1450°C to
153 1500°C for 6 hours and subsequent air cooling. MCPM was synthesized by slowly
154 mixing calcium carbonate into an acetone solution with phosphoric acid for 15 minutes.
155 The mixture solution was kept for 30 minutes and washed with deionized water to
156 remove unreacted phosphate ions. Finally, the MCPM powder was obtained after drying
157 for 24 hours.

158 The premix TTCP/MCPM was comminuted in a laboratory ball mill BLT-100 (JIN-
159 BOMB ENTERPRISE CO., LTD.) containing an ethanol (>95.0%, VWR) suspension.
160 Milling beads with diameters of 10 mm and 5 mm were used in a 1:1.5 ratio by weight.

The rotating speed of the ball mill was 400~500 rpm for 24 hours. Powder recovery was done by centrifugation and subsequent drying at 80°C for 24 hours in a muffle furnace (Nabertherm). A schematic diagram of the sample preparation process is shown in Fig. 1.

Preparation of TTCP/MCPM sponge

The different ratios (1:1, 1.1:1, 2:1, 3.5:1, 5:1, and 10:1) of TTCP and MCPM powders were mixed with 0.1 wt% magnesium, then Type I Collagen solution (0.3 ug/ml) (Cat. No. CLS354236; Corning, New York, U.S.A.) was employed as coating reagent. The powder-to-collagen weight ratio was maintained at 1:3, and the mixture was subjected to magnetic stirring.

Subsequently, the TTCP/MCPM powder mixed with Collagen solution was poured into molding molds. The molds were then placed in a -20℃ for 2 hours. After complete solidification of the composite block, it was transferred to a freeze-dryer for overnight freeze-drying, and a porous composite material (TTCP/MCPM/Collagen) was obtained.

Scanning electron microscopy (SEM)

Particle size and degree of agglomeration were analyzed by scanning electron microscopy (Gemini Ultra 55, Carl Zeiss). The submicron particles were prepared by

178 embedding powders in a conductive paste. Secondary electrons were used for imaging
179 at an accelerating voltage of 2 kV [26].

180 ***Dynamic light scattering (DLS)***

181 Size distributions of powders were determined by dynamic light scattering at a
182 wavelength of 632.8 nm (DLS, model DLS-700, Otsuka Electronics Co., Osaka, Japan).
183 Samples for the DLS measurements were prepared by dispersing small amounts of the
184 powder in ethanol (filtered using a 0.2 μm filter), followed by treatment in an ultrasonic
185 bath for 10 min. After transferring to the sample holder, the suspensions were diluted
186 again using filtered ethanol and ultrasonicated for 3 min. The measurement conditions
187 included a sampling time of 80 μs and 100 accumulations. A viscosity of 1.19 cP and a
188 refractive index of 1.36 was used for calculations [27].

189 ***X-ray diffraction spectroscopy (XRD)***

190 XRD was conducted to examine the crystal phase composition of the samples. A 0.5mm
191 × 0.5mm area of each sample was randomly selected, and the XRD spectra were
192 acquired at room temperature using an X-ray diffractor (D/max-II; RIGAKU, Japan)
193 with Cu Kα radiation. The range was 10–90° with a 0.2° step and 1 s/step scan speed
194 (40 kV, 40 mA).

Cell culture

The murine osteoblast cell line MC3T3-E1, osteoclast precursor cell line RAW264.7, and human umbilical vein endothelial cells (HUVEC) were obtained from the American Type Culture Collection (ATCC; Manassas, VA, USA). The MC3T3-E1 and RAW264.7 cells were maintained in complete media including alpha-minimal essential medium (α-MEM) supplemented with streptomycin (100 μg/mL), penicillin (100 U/mL), and 10% fetal bovine serum (FBS). The HUVEC cells were maintained in EBM-2 media (Lonza) supplemented with streptomycin (100 μg/mL), penicillin (100 U/mL), and 20% FBS. All cells were kept at 37 °C in an atmosphere of humidified air with 5% CO_2 [28].

Cell proliferation

Cell proliferation was detected by the 3-(4,5-dimethylthiazol-2-yl)-2,5-diphenyltetrazolium bromide (MTT) assay as previously described [29]. MC3T3-E1 and RAW264.7 cells seeded on different synthetic materials were kept in 96-well plates for 1 or 3 days. The cells were rinsed with PBS, followed by incubation with MTT (0.5 mg/mL) at 37 °C for 2 h. Two hours later, cells were lysed by DMSO to dissolve formazan crystals [30]. After the mixture was shaken at room temperature (RT) for 10 min, the absorbance of each well was determined at 450 nm using a microplate (ELISA) reader (Bio-Tek, Winooski, VT, USA).

Osteoblast differentiation

The MC3T3-E1 osteoblasts grown in different CPC sponges have been further assessed for their differentiation by alkaline phosphatase (ALP) activity assay (Alkaline Phosphatase Activity Assay Kit (C); BioVision, wavelengths: 405nm, extract) [31]. The cells were incubated with different CPC sponges for 3 days. The incubated cells were rinsed twice with PBS, followed by the collection of total cell lysate using a lysis buffer. The cell lysates were subjected to the measurement of alkaline phosphatase (ALP) activity.

Osteoblast mineralization

The MC3T3-E1 osteoblasts were differentiated in an induction medium containing vitamin C (50 μg/mL), and β-glycerophosphate (10 mM) for 2 weeks as the previous report described [32]. Cells were fixed in ice-cold 75% (v/v) ethanol for 30 min, and the calcium deposition was determined using 40 mM alizarin red-S staining (pH 4.2) (Sigma–Aldrich, 405nm, extract).

Osteoclast differentiation

Osteoclast differentiation was performed as previously described [32]. Briefly, RAW264.7 osteoclast precursor cells were differentiated to osteoclasts in Dulbecco's

230 modified Eagle's medium supplemented with 10% FBS, 100 U/ml penicillin, and 100
231 μg/ml streptomycin for 7 days. All cells were incubated with macrophage colony-
232 stimulating factor (M-CSF) (20 ng/ml) and RANKL (50 ng/ml) and incubated with
233 different CPC sponges. Finally, osteoclast differentiation was detected by tartrate-
234 resistant acid phosphatase activity (TRAP; Acid Phosphatase Kit 387-A; Sigma–
235 Aldrich, no extract) according to the manufacturer's instructions. The absorbance was
236 measured at 405 nm using a microplate reader.

237 ***Endothelial Cell Tube Formation Assay***

238 HUVEC (3×10^4 cells) were seeded onto pre-coated Matrigel plates (BD Biosciences,
239 Bedford, MA), which were premixed with synthetic materials. The formation of EC
240 tubes was photographed and tube branches were calculated using MacBiophotonics
241 Image J software [33, 34].

242 ***Ferrous ion chelating assay***

243 For the antioxidant activity test, briefly, the synthetic materials were mixed with 5 μL
244 of 2 mM ferrous chloride ($FeCl_2$). The reaction was initiated by the addition of 10 μL
245 of 5 mM ferrozine. After 10 min at room temperature, the Abs. was determined at 562
246 nm using a microplate reader (Dynex Technologies, Inc., Chantilly, VA, US).

Statistical analysis

The statistical analysis was performed using SPSS Statistics 20. All data are presented as the mean ± SD and were analyzed by one-way ANOVA. Bonferroni correction was used for post hoc comparisons.

Results

Sedimentation of sub-micron particles

The experiments involved the assessment of synthetic sub-micron particle suspensions with varying average sizes, facilitating an exploration of the sample's behavior within the medium. Suspensions were created by introducing particles of distinct diameters (1 mm, 3.5, and 0.35 μm) into water. The outcomes of these experiments are depicted in Figure 2A.

SEM observation of TTCP/MCPM particles

SEM was used to evaluate the morphology of a synthetic material, TTCP/MCPM powder. As shown in (Fig. 2A), the macroscopic morphologies of the images indicate the average size of particles was in the submicron to lower micron range after milling, compared with the original raw material (> 3 mm).

Dynamic light scattering

The particle size distributions (PSD) of our synthetic material were analyzed by DLS (Fig. 2C). The PSD result showed the average size distribution decreased to 328.7 nm after milling. More than 95% of the particles were sub-micron in diameter.

Setting time and compressive strength

The influence of different TTCP/MCPM ratios on the setting time of CPCs is listed in (Table 1). The results showed that TTCP/MCPM ratios of 1:1 and 1.1:1 could not form hard CPC sponges properly, even for more than 30 min. The CPC sponge, on the other hand, begins to form when the TTCP/MCPM ratio increases to 2:1, with a setting time of more than 20 min and soft compressive strength (1.09±0.36MPa). We also found that the TTCP/MCPM ratio of 3.5:1 had an appropriate compressive strength (4.39 ± 0.96 MPa) within 15 min, which is comparable to human spongy bone strength. Despite the higher compressive strength (4.66 ± 1.31 MPa) of the group with a TTCP/MCPM ratio of 5:1, the setting time was too short for clinical procedures. Moreover, the group with a TTCP/MCPM ratio of 10:1 couldn't even form a cohesive structure. Therefore, the TTCP/MCPM ratio of 3.5:1 exhibited the most suitable properties for clinical applications.

SEM observation of CPC sponge with collagen covering

The macroscopic morphologies show that collagen uniformly covered the surface of the CPC sponge (Fig. 2B(i)). After being provided with a hardening accelerator (Na_2HPO_4, glycerol, and citrate), the CPC sponge exhibits a similar structure, with tinny mineral crystals of collagen fibers dispersing homogeneously on the surface of the CPC sponge (Fig. 2B(ii)).

XRD analysis

The CPC sponge, derived from TTCP and MCPM, ultimately transforms into hydroxyapatite (HA) during its formation. To confirm this characteristic, XRD analysis was conducted post-reaction of the CPC sponge. As depicted in Fig. 2D, the XRD patterns revealed distinct peaks for the synthesized CPC sponge at angles of 25.9° (002), 31.8° (211), 32.9° (300), 34.0° (202), 39.8° (310), 46.7° (222), 49.5° (213), and 53.1° (004). These angles align closely with those of standard HA.

***In vitro* biocompatibility test of different CPC sponges**

The cell viability on the CPC sponge can show the cytotoxicity and biocompatibility of the synthetic materials. Therefore, the MTT assay was used to investigate the viability of two different bone cells, osteoblasts, and osteoclasts on different CPC sponges. The results revealed that CPC sponges had a beneficial effect on MC3T3-E1 osteoblasts

viability, as provided in (Fig. 3A). The CPC sponges inhibited cell viability by approximately 30 % in osteoclast precursors RAW264.7 at a high concentration (0.2 g/mL; Fig. 3B).

Chelation power of different CPC sponges

The results indicated that all CPC sponges could chelate ferrous ions, and interestingly, CPC sponges containing magnesium possessed more significant chelation power than other materials, especially at a high concentration (0.2 g/mL; Fig. 4).

Osteoblast proliferation, differentiation, and mineralization assays of different CPC sponges

To evaluate the capacity of the CPC sponge for bone repair and regeneration, we investigated the proliferation, differentiation, and mineralization in osteoblasts on different CPC sponges. There was a significant difference between CPC sponges on osteoblasts proliferation compared with the control group (Fig. 5A). In the osteoblast differentiation assay, the data showed that the CPC sponge containing magnesium exhibited great potential to promote osteoblast differentiation after 3-day incubation, as monitored by the ALP activity assay (Fig. 5B). Finally, the mineralization assay, which was accomplished by detecting calcium deposition, demonstrated that the CPC sponge

315 containing magnesium increased osteoblast mineralization as well (Fig. 5C and 5D).

316 **Osteoclast differentiation assay of different CPC sponges**

317 The osteoclast differentiation was conducted by TRAP activity assay, and the result
318 indicated that incubation with different CPC sponges did not increase osteoclast
319 differentiation compared with the positive control (RANKL+MCSF group; Fig. 6).
320 Instead, these synthetic materials showed inhibition of osteoclasts differentiation.

321 **Angiogenesis assay of different CPC sponges**

322 The result found that the CPC sponge contained magnesium had more tube-like
323 morphology than other synthetic materials (Fig. 7), which reveals magnesium released
324 from the CPC sponge may improve wound healing as well as bone regeneration.

325 # Discussions

326 Our study indicates the synthetic particle with a 0.35 μm sub-micron size generated
327 white colloidal dispersions, suggesting sedimentation rate is greatly influenced by
328 extra-fine particle size. We also successfully established a reliable synthetic process by
329 wet comminution in stirred media mills to produce sub-micron particles. The
330 TTCP/MCPM ratio of 3.5:1 had the highest compressive strength (4.39 ± 0.96 MPa)
331 within 15 min, which is comparable to human spongy bone strength. The results

indicate that a CPC sponge composed of TTCP/MCPM and collagen covering could produce the same crystalline structure of HA. The biocompatibility of CPC was evaluated in vitro by the MTT test and by the analysis of cell morphology of the MC3T3-E1 and RAW264.7 cultured in direct contact with CPC. *In vitro,* biocompatibility tests showed that magnesium could promote osteoblast viability, in agreement with previous reports [22-24]. Chelation power on ferrous ions, referring to in vitro antioxidant capacity, revealed CPC sponges containing magnesium possessed more significant chelation power than other materials, especially in a high concentration. In agreement with a previous study [35], the evidence proved that magnesium released from the CPC sponge could enhance osteoblast activity. Besides, our study reveals that CPC sponges may improve bone regeneration by targeting osteoclasts [6, 36]. Magnesium was implicated in modulating microvascular functions, including angiogenesis, considered a critical process in bone regeneration [37].

Improvement of bioactivity and biocompatibility of bone-graft substitutes in clinical applications such as bone regeneration is an unmet need [38, 39]. An increase in the biological function of various cells, for example, osteoblasts, osteoclasts, and endothelial cells resident in the fracture healing region, usually improves transplantation efficiency. Therefore, a fundamental understanding of the cell response

to different synthetic materials is key to the development of novel biomaterials. Here, we demonstrate the effects of a sub-micron CPC sponge containing magnesium on various cell types that were required for bone regeneration, for example, osteoblasts, osteoclasts, and endothelial cells. The results provide promising benefits for this novel CPC sponge in bone regeneration. Plenty of evidence has shown nanoscale particles could improve the bioactivity of different biomaterials [40]. Bone is an organ composed of approximately 60% mineral, mostly nano-hydroxyapatite, which is almost identified with calcium phosphate (CaP) ceramic [41]. Tricalcium phosphate (TCP) is one major form of CaP ceramic used in bone regeneration clinically. The ion-containing TCPs are also produced to promote specific biological functions. For example, TCP-based magnesium-containing material was proven to enhance bone healing by modulating osteogenesis and angiogenesis in an animal model [42, 43], with increasing compressive strength than pure TCP scaffolds. However, TCP ceramics have limitations caused by poor mechanical properties [40]. In our current study, we introduced a novel sub-micron CaP material consisting of TTCP/MCPM. This material has morphology and biomechanical properties comparable to the nature of bone due to the needle-like HA structure that formed on the surface of the material after implantation. Our synthetic sub-micron CaP material also exhibited better biocompatibility than the original size of

368 CaP, which agrees with the previous findings (Appendix 1).

369 Data obtained from the in vitro experiments prove that the CPC sponge containing
370 magnesium has the capacity to promote osteoblast differentiation and mineralization.
371 Previous reports have proven that magnesium ions in the culture medium enhanced the
372 adhesion and stimulated the osteogenic differentiation of cells [44-46]. Furthermore,
373 several studies have developed magnesium/calcium phosphate types of cement (MCPC)
374 by different procedures [47-49]. In Zhang et al. report, they found that MCPC with a
375 moderate proportion of MPC (5% and 10%, referred to as 5MCPC and 10MCPC) were
376 found to strongly enhance adhesion and osteogenic differentiation of bone marrow
377 stromal cells [49]. Interestingly, this effect was accomplished by direct interaction of
378 fibronectin, integrin α5β1, and magnesium ions on the scaffold, but not by the released
379 magnesium ions. Our present work develops a novel sub-micron MCPC sponge for the
380 first time. We also found that higher magnesium concentrations (0.2 g/mL) induced
381 osteoblast proliferation significantly. The role of angiogenesis in bone regeneration has
382 been well discussed [37]. Thomas E. Paterson et al. found that porous microspheres, an
383 injectable bone filler, have the potential to stimulate angiogenesis [50]. Our results also
384 prove a sub-micron MCPC sponge could promote the tube-like formation of HUVEC
385 cells. Claudia S. Oliveira et al. emphasized the potential of bioengineered bone

386 microenvironments to facilitate the process of bone regeneration [51]. This evidence
387 showed that this synthetic material was able to modulate multiple biological functions
388 during bone regeneration. However, the proper concentration of magnesium used in this
389 sub-micron CPC sponge should be certified in the future.

390 **Conclusion**

391 The current study generates sub-micron particles composed of TTCP/MCPM powder
392 and uses wet comminution in stirred media mills, which is a synthetic process. After
393 covering it with collagen and magnesium to produce a CPC sponge, we evaluated the
394 material's structural characteristics as well as biocompatibility in different cell types.
395 Our results show that a CPC sponge containing magnesium has great potential to
396 improve osteoblasts and endothelial cell functions with minimal cytotoxicity effects.
397 Our findings pave the way for upcoming endeavors to employ CPC sponge composite
398 for in vivo applications in a clinical setting.

399 **Conflict of Interest**

400 The authors have no conflicts to disclose

401 **Acknowledgments**

402 Yuan-Hsin Tsai carried out his thesis research under the auspices of the Ph.D. Program
403 in Tissue Engineering and Regenerative Medicine, National Chung Hsing University,
404 and National Health Research Institutes. We thank Li-Heng Liu for their helpful

assistance and support. This research was supported by the Ministry of Science and Technology, Taiwan for the grants (MOST 110-2221-E-005-010, MOST 111-2221-E-005-009, and MOST 111-2221-E-005 -026 -MY3). We also thank National Chung Hsing University (ENABLE: 108ST001B and 110ST001G), Kasesart University Joint Research Project (108RA129A), and NCHU-MIRDC Bilateral Joint Research Project (110S0703B).

Contact for reagent and resource sharing

Further information and requests for reagents should be directed to Lead Contact Hui-Ming David Wang (davidw@dragon.nchu.edu.tw)

Data Availability

The data used to support the findings of this study are available from the corresponding author upon request.

References

[1] Dimitriou R, Jones E, McGonagle D, Giannoudis PV. Bone regeneration: current concepts and future directions. BMC Medicine 2011;9:66.

[2] Migliorini F, La Padula G, Torsiello E, Spiezia F, Oliva F, Maffulli N. Strategies for large bone defect reconstruction after trauma, infections or tumour excision: a comprehensive review of the literature. Eur J Med Res 2021;26(1):118.

[3] Wang W, Yeung KWK. Bone grafts and biomaterials substitutes for bone defect repair: A review. Bioact Mater 2017;2(4):224-47.

[4] Stahl A, Yang YP. Regenerative Approaches for the Treatment of Large Bone Defects. Tissue Eng Part B Rev 2021;27(6):539-47.

[5] Sen M, Miclau T. Autologous iliac crest bone graft: should it still be the gold standard for treating nonunions? Injury 2007;38(1):S75-S80.

[6] Huang EE, Zhang N, Ganio EA, Shen H, Li X, Ueno M, et al. Differential dynamics of bone graft transplantation and mesenchymal stem cell therapy during bone defect healing in a murine critical size defect. J Orthop Transl. 2022;36:64-74.

[7] Giannoudis PV, Einhorn TA. Bone morphogenetic proteins in musculoskeletal medicine. Injury 2009;40 Suppl 3:S1-3.

[8] Myeroff C, Archdeacon M. Autogenous bone graft: donor sites and techniques. JBJS 2011;93(23):2227-36.

[9] Jeong C-H, Kim J, Kim HS, Lim S-Y, Han D, Huser AJ, et al. Acceleration of bone formation by octacalcium phosphate composite in a rat tibia critical-sized defect. J Orthop Translat 2022;37:100-12.

[10] Makhdom AM, Hamdy RC. The role of growth factors on acceleration of bone regeneration during distraction osteogenesis. Tissue Eng Part B, Rev 2013;19(5):442-53.

[11] Heckman JD, McKee M, McQueen MM, Ricci W, Tornetta III P. Rockwood and Green's fractures in adults. Lippincott Williams & Wilkins; 2014.

[12] Bauer TW, Muschler GF. Bone graft materials. An overview of the basic science. Clin Orthop Relat Res 2000(371):10-27.

[13] Laubach M, Suresh S, Herath B, Wille M-L, Delbrück H, Alabdulrahman H, et al. Clinical translation of a patient-specific scaffold-guided bone regeneration concept in four cases with large long bone defects. J Orthop Translat 2022;34:73-84.

[14] De Long WG, Jr., Einhorn TA, Koval K, McKee M, Smith W, Sanders R, et al. Bone grafts and bone graft substitutes in orthopaedic trauma surgery. A critical analysis. J Bone Joint Surg Am volume 2007;89(3):649-58.

[15] Centers for Disease C. Transmission of HIV through bone transplantation: case report and public health recommendations. MMWR Morb Mortal Wkl Rep 1988;37(39):597-9.

[16] Stevenson S, Horowitz M. The response to bone allografts. J Bone Joint Surg Am volume 1992;74(6):939-50.

[17] Kurien T, Pearson RG, Scammell BE. Bone graft substitutes currently available in orthopaedic practice: the evidence for their use. Bone Joint J 2013;95-B(5):583-97.

[18] Lindley TE, Dahdaleh NS, Menezes AH, Abode-Iyamah KO. Complications associated with recombinant human bone morphogenetic protein use in pediatric craniocervical arthrodesis. J Neurosurg Pediatr 2011;7(5):468-74.

[19] Jahnen-Dechent W, Ketteler M. Magnesium basics. Clin Kidney J 2012;5(Suppl 1):i3-i14.

[20] Belluci MM, Schoenmaker T, Rossa-Junior C, Orrico SR, de Vries TJ, Everts V. Magnesium deficiency results in an increased formation of osteoclasts. The J Nutr Biochem 2013;24(8):1488-98.

[21] Diaz-Tocados JM, Herencia C, Martinez-Moreno JM, Montes de Oca A, Rodriguez-Ortiz ME, Vergara N, et al. Magnesium Chloride promotes Osteogenesis through Notch signaling activation and expansion of Mesenchymal Stem Cells. Sci Rep 2017;7(1):7839.

475 [22] Farraro KF, Kim KE, Woo SL, Flowers JR, McCullough MB. Revolutionizing
476 orthopaedic biomaterials: The potential of biodegradable and bioresorbable
477 magnesium-based materials for functional tissue engineering. J Biomech
478 2014;47(9):1979-86.

479 [23] Kraus T, Fischerauer SF, Hanzi AC, Uggowitzer PJ, Loffler JF, Weinberg AM.
480 Magnesium alloys for temporary implants in osteosynthesis: in vivo studies of
481 their degradation and interaction with bone. Acta Biomater 2012;8(3):1230-8.

482 [24] Witte F, Kaese V, Haferkamp H, Switzer E, Meyer-Lindenberg A, Wirth CJ, et
483 al. In vivo corrosion of four magnesium alloys and the associated bone response.
484 Biomaterials 2005;26(17):3557-63.

485 [25] Liu J, Hou W, Wei W, Peng J, Wu X, Lian C, et al. Design and fabrication of
486 high-performance injectable self-setting trimagnesium phosphate. Bioact Mater
487 2023;28:348-57.

488 [26] Chang WT, Wu CY, Lin YC, Wu MT, Su KL, Yuan SS, et al. C(2)-Ceramide-
489 Induced Rb-Dominant Senescence-Like Phenotype Leads to Human Breast
490 Cancer MCF-7 Escape from p53-Dependent Cell Death. Int J Mol Sci
491 2019;20(17).

[27] Nguyen NT-P, Nguyen LV-H, Thanh NT, Toi VV, Ngoc Quyen T, Tran PA, et al. Stabilization of silver nanoparticles in chitosan and gelatin hydrogel and its applications. Mat Lett 2019;248:241-5.

[28] Lin R-H, Hung H-S, Tang C-M, Tsou H-K, Chen P-H, Yueh C-Y, et al. In vitro biocompatibility of polycaprolactone/hydroxyapatite nanocomposite membranes modified by oleic acid for bone regeneration. Colloids Surf A: Physicochem Eng Asp 2024;688:133576.

[29] Chen PC, Cheng HC, Wang J, Wang SW, Tai HC, Lin CW, et al. Prostate cancer-derived CCN3 induces M2 macrophage infiltration and contributes to angiogenesis in prostate cancer microenvironment. Oncotarget 2014;5(6):1595-608.

[30] Nail HM, Chiu CC, Leung CH, Ahmed MMM, Wang HD. Exosomal miRNA-mediated intercellular communications and immunomodulatory effects in tumor microenvironments. J Biomed Sci 2023;30(1):69.

[31] Izumiya M, Haniu M, Ueda K, Ishida H, Ma C, Ideta H, et al. Evaluation of MC3T3-E1 Cell Osteogenesis in Different Cell Culture Media. Int J Mol Sci 2021;22(14).

[32] Chen PC, Cheng HC, Tang CH. CCN3 promotes prostate cancer bone metastasis by modulating the tumor-bone microenvironment through RANKL-dependent pathway. Carcinogenesis 2013;34(7):1669-79.

[33] Su CM, Hsu CJ, Tsai CH, Huang CY, Wang SW, Tang CH. Resistin Promotes Angiogenesis in Endothelial Progenitor Cells Through Inhibition of MicroRNA206: Potential Implications for Rheumatoid Arthritis. Stem cells 2015;33(7):2243-55.

[34] Chen CY, Su CM, Hsu CJ, Huang CC, Wang SW, Liu SC, et al. CCN1 Promotes VEGF Production in Osteoblasts and Induces Endothelial Progenitor Cell Angiogenesis by Inhibiting miR-126 Expression in Rheumatoid Arthritis. JBMR: The official J ASBMR 2017;32(1):34-45.

[35] Castiglioni S, Cazzaniga A, Albisetti W, Maier JA. Magnesium and osteoporosis: current state of knowledge and future research directions. Nutrients 2013;5(8):3022-33.

[36] Lee HP, Lin YY, Duh CY, Huang SY, Wang HM, Wu SF, et al. Lemnalol attenuates mast cell activation and osteoclast activity in a gouty arthritis model. J Pharm Pharmacol 2015;67(2):274-85.

[37] Wang M, Yu Y, Dai K, Ma Z, Liu Y, Wang J, et al. Improved osteogenesis and angiogenesis of magnesium-doped calcium phosphate cement via macrophage immunomodulation. Biomater Sci 2016;4(11):1574-83.

[38] Cai P, Lu S, Yu J, Xiao L, Wang J, Liang H, et al. Injectable nanofiber-reinforced bone cement with controlled biodegradability for minimally-invasive bone regeneration. Bioact Mater 2023;21:267-83.

[39] Seifert A, Tylek T, Blum C, Hemmelmann N, Böttcher B, Gbureck U, et al. Calcium phosphate-based biomaterials trigger human macrophages to release extracellular traps. Biomaterials 2022;285:121521.

[40] Lyons JG, Plantz MA, Hsu WK, Hsu EL, Minardi S. Nanostructured Biomaterials for Bone Regeneration. Front Bioeng Biotechnol 2020;8:922.

[41] Minardi S, Corradetti B, Taraballi F, Sandri M, Van Eps J, Cabrera FJ, et al. Evaluation of the osteoinductive potential of a bio-inspired scaffold mimicking the osteogenic niche for bone augmentation. Biomaterials 2015;62:128-37.

[42] Bose S, Tarafder S, Banerjee SS, Davies NM, Bandyopadhyay A. Understanding in vivo response and mechanical property variation in MgO, SrO and SiO(2) doped beta-TCP. Bone 2011;48(6):1282-90.

543 [43] Tarafder S, Dernell WS, Bandyopadhyay A, Bose S. SrO- and MgO-doped
544 microwave sintered 3D printed tricalcium phosphate scaffolds: mechanical
545 properties and in vivo osteogenesis in a rabbit model. J Biomed Mater Res B
546 Appl Biomater 2015;103(3):679-90.

547 [44] Yoshizawa S, Brown A, Barchowsky A, Sfeir C. Role of magnesium ions on
548 osteogenic response in bone marrow stromal cells. Connect Tissue Res 2014;55
549 Suppl 1:155-9.

550 [45] Wu L, Feyerabend F, Schilling AF, Willumeit-Romer R, Luthringer BJC.
551 Effects of extracellular magnesium extract on the proliferation and
552 differentiation of human osteoblasts and osteoclasts in coculture. Acta Biomater
553 2015;27:294-304.

554 [46] Yoshizawa S, Brown A, Barchowsky A, Sfeir C. Magnesium ion stimulation of
555 bone marrow stromal cells enhances osteogenic activity, simulating the effect
556 of magnesium alloy degradation. Acta Biomater 2014;10(6):2834-42.

557 [47] Jia J, Zhou H, Wei J, Jiang X, Hua H, Chen F, et al. Development of magnesium
558 calcium phosphate biocement for bone regeneration. J R Soc Interface
559 2010;7(49):1171-80.

[48] Goldberg MA, Krohicheva PA, Fomin AS, Khairutdinova DR, Antonova OS, Baikin AS, et al. Insitu magnesium calcium phosphate cements formation: From one pot powders precursors synthesis to in vitro investigations. Bioact Mater 2020;5(3):644-58.

[49] Zhang J, Ma X, Lin D, Shi H, Yuan Y, Tang W, et al. Magnesium modification of a calcium phosphate cement alters bone marrow stromal cell behavior via an integrin-mediated mechanism. Biomaterials 2015;53:251-64.

[50] Paterson TE, Gigliobianco G, Sherborne C, Green NH, Dugan JM, MacNeil S, et al. Porous microspheres support mesenchymal progenitor cell ingrowth and stimulate angiogenesis. APL Bioeng 2018;2(2):026103.

[51] Oliveira CS, Leeuwenburgh S, Mano JF. New insights into the biomimetic design and biomedical applications of bioengineered bone microenvironments. APL Bioeng 2021;5(4):041507.

Figure legends

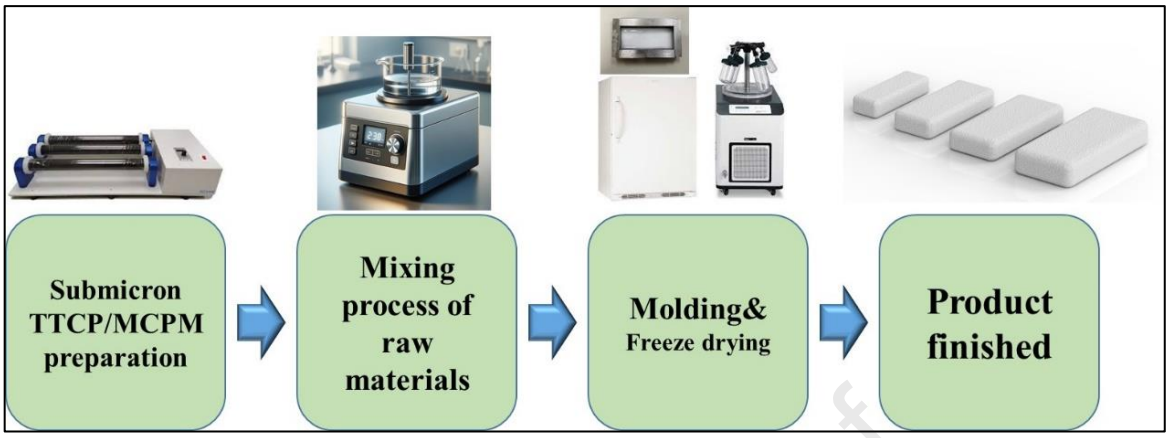

Fig. 1 Schematic diagram of the sample preparation process.

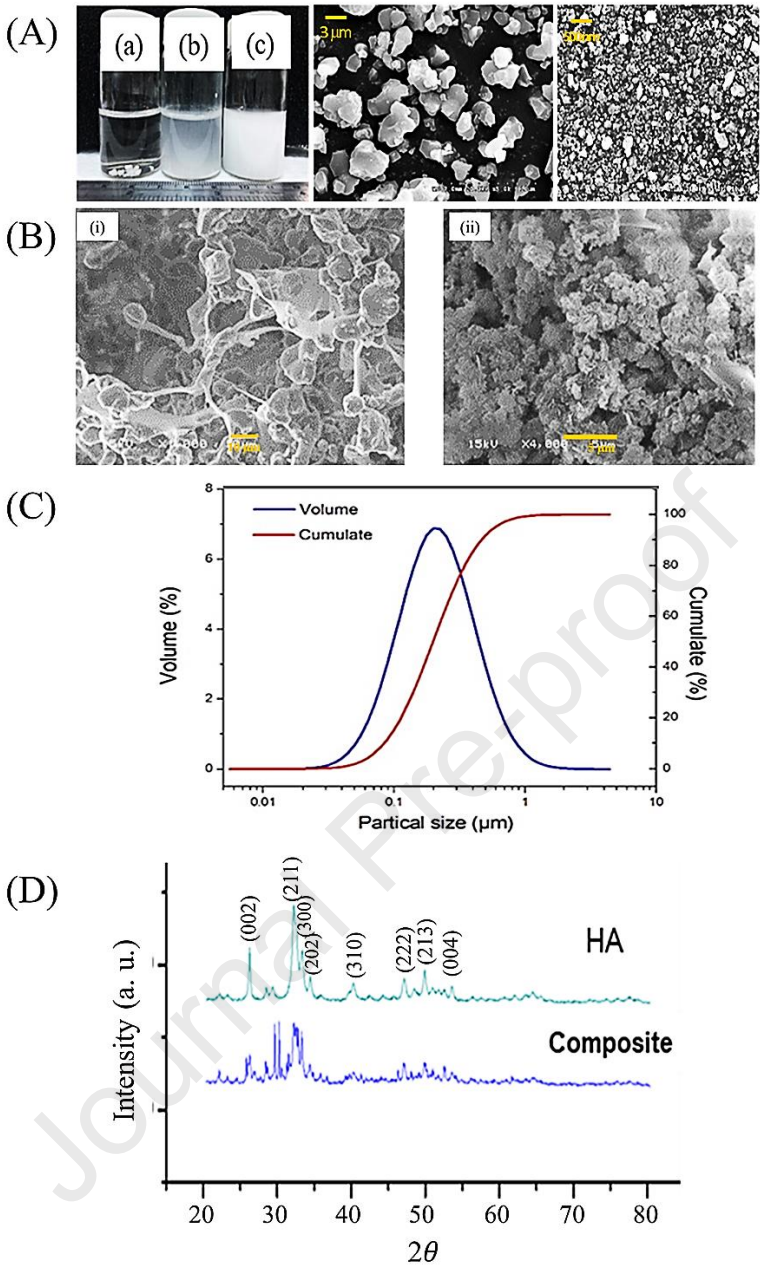

Fig. 2 Characterization of CPC powder. (**A**) (left) Sedimentation behavior modes of suspensions of different sub-micron CPC powder (5 mg/mL). (a) 1 mm, (b) 3.5 μm, (c) 0.35 μm. The SEM image of original feed CPC powder (middle) and sub-micron CPC powder after milling (right). (**B**) SEM images of surfaces of the sub-micron CPC sponge covered by collagen. The sub-micron CPC sponge is covered by collagen before (i) and after hardening (ii). (**C**) Particle size distributions of the sub-micron CPC powder by DLS (cumulative distributions were shown as red line). (**D**) X-ray diffraction patterns of the hydroxyapatite (HA) and sub-micron CPC sponge (composite) after hardening.

604

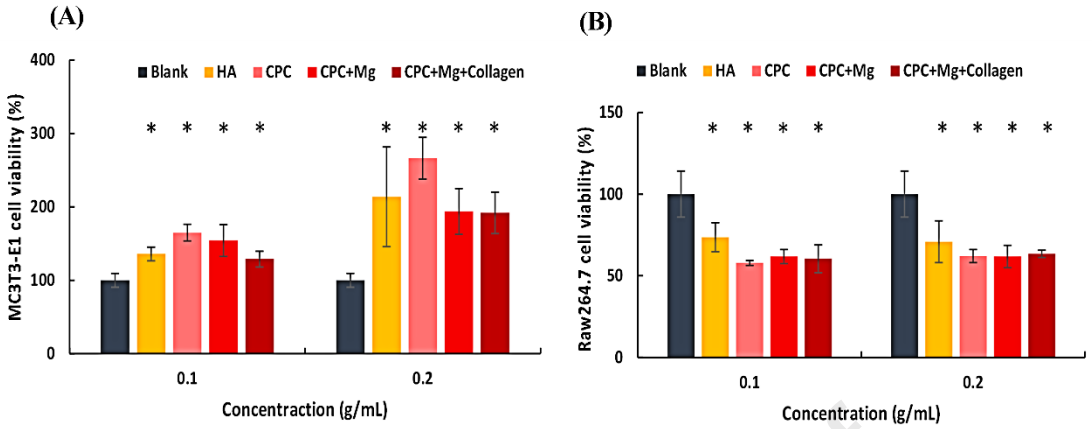

605

606 Fig. 3 MTT assay of MC3T3-E1 and RAW264.7 cell lines incubated with sub-micron
607 CPC sponges (CPC + Mg + Collagen). The cells were incubated with different
608 concentrations (0.1 and 0.2 g/mL) of various CPC sponges. The cell viability assays
609 were conducted by MTT in MC3T3-E1 osteoblasts (A) and RAW264.7 osteoclast
610 precursor cells (B). (one-way ANOVA, mean ± SD, n=6, *p < 0.05 compared with
611 blank).

612

613

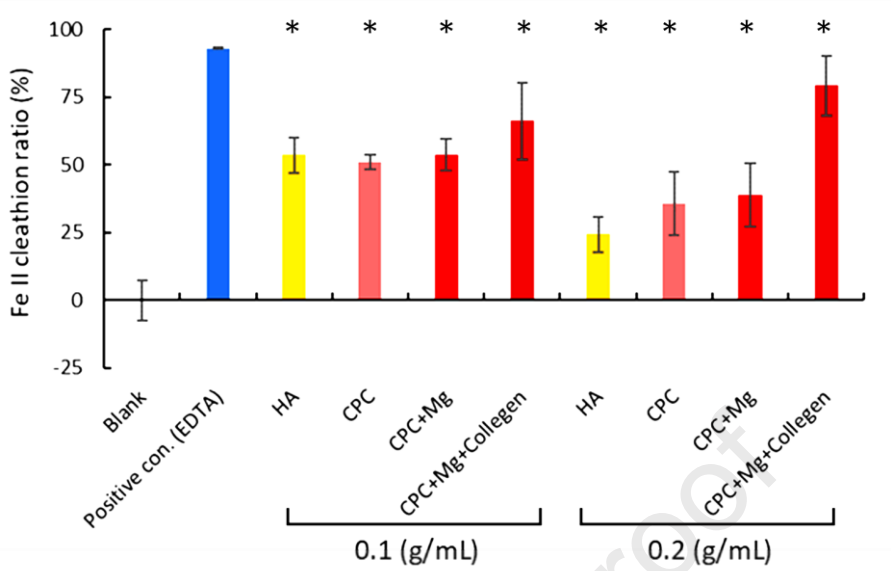

614

615 Fig. 4 Chelation power on ferrous ions of sub-micron CPC sponges (CPC + Mg +
616 Collagen). (one-way ANOVA, mean ± SD, n=6, *p < 0.05 compared with blank).
617 EDTA: 100μM
618

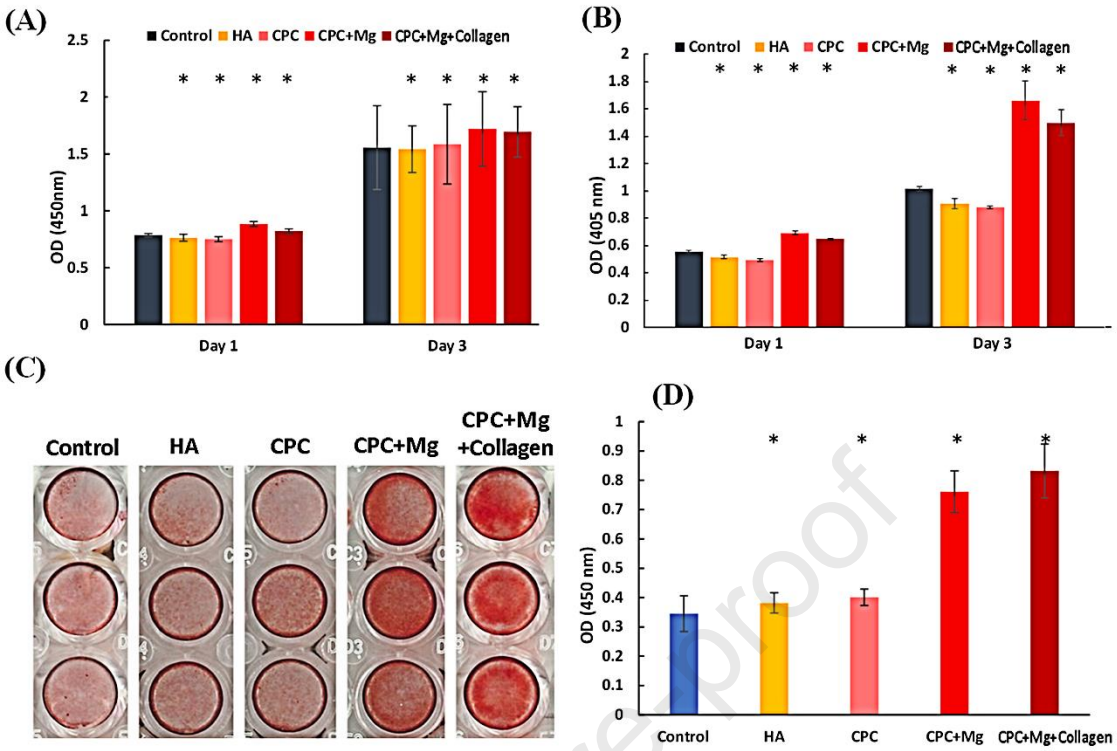

Fig. 5 Effects of sub-micron CPC sponges (CPC + Mg + Collagen) on proliferation, differentiation, and mineralization in MC3T3-E1 osteoblasts. The MC3T3-E1 osteoblasts were incubated with different sub-micron CPC sponges for 3 days. The cell proliferation on day 1 and day 3 (A), cell differentiation on day 1 and day 3 (B), and mineralization as calcium deposition (C), and mineralization (D) were determined. (one-way ANOVA, mean ± SD, n=6, *$p < 0.05$ compared with blank).

628

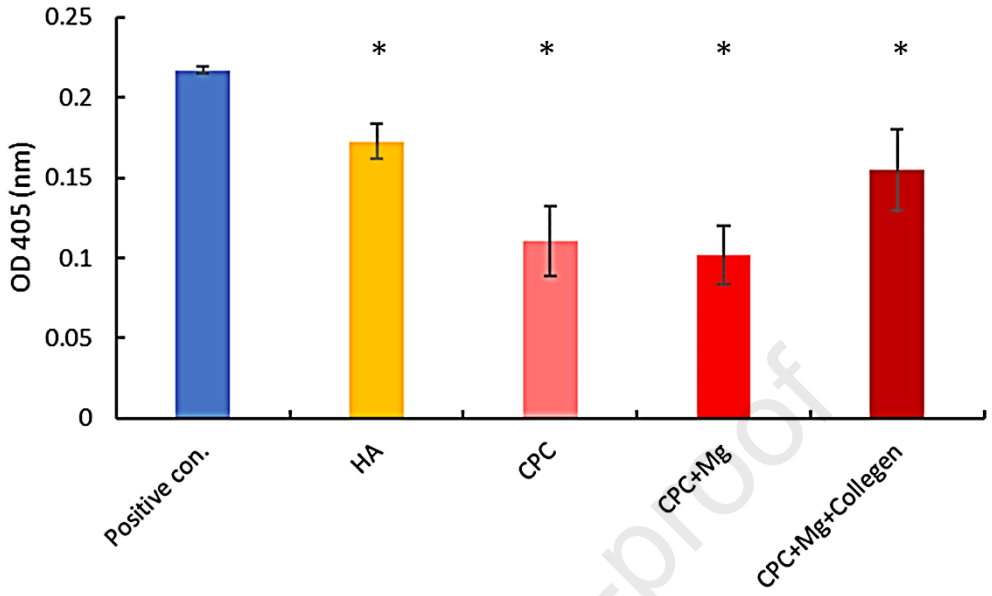

629

630 Fig. 6 Effects of sub-micron CPC sponges (CPC + Mg + Collagen) on osteoclast
631 differentiation. The RAW264.7 osteoclast precursor cells were incubated with different
632 sub-micron CPC sponges for 7 days. The osteoclast differentiation was analyzed by a
633 TRAP activity assay. (one-way ANOVA, mean ± SD, n=6, *p < 0.05 compared with
634 blank).
635 EDTA: 100μM
636

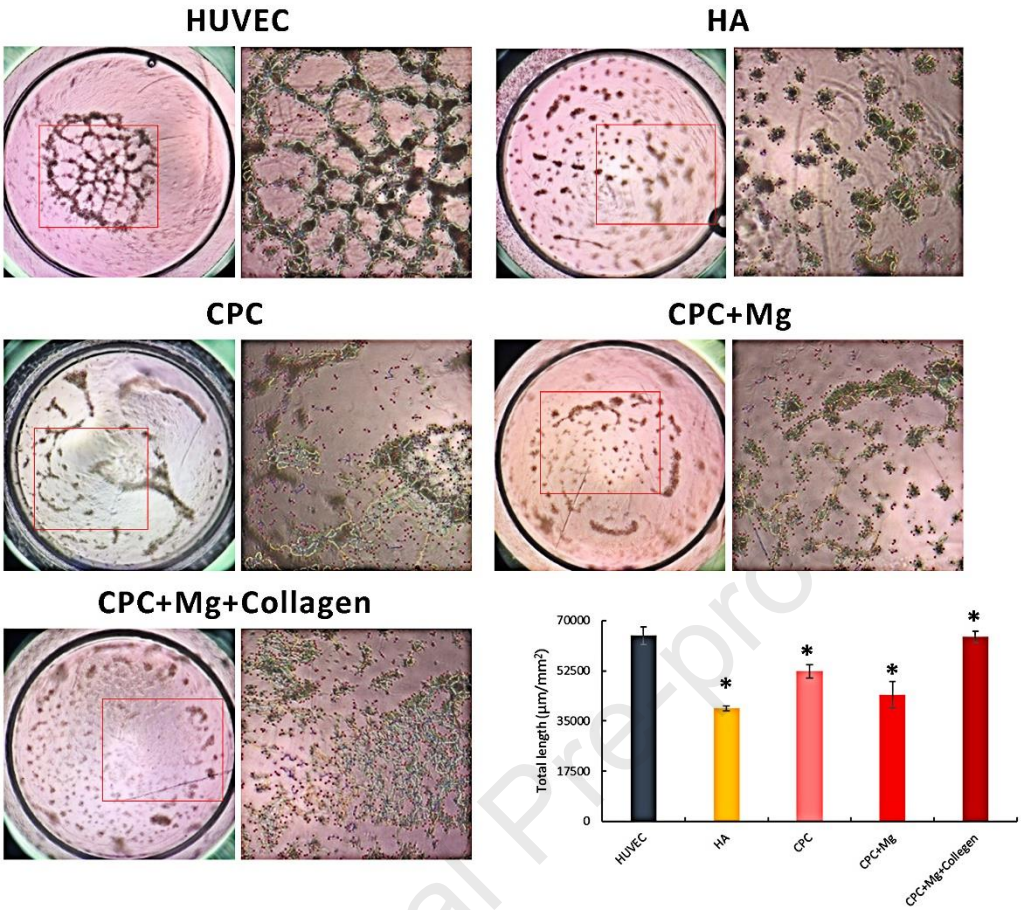

Fig. 7 Effects of sub-micron CPC sponges on angiogenesis. The HUVEC endothelial cells were incubated with different sub-micron CPC sponges for 12 hr. The tube-like structure was monitored by a microscope and the number of cells per field was counted. (one-way ANOVA, mean ± SD, n=6, *p < 0.05 compared with blank).

644 **Table 1**. Properties of different ratios of sub-micron CPC sponges.
645

Properties of different ratios of sub-micron CPC (TTCP/MCPM) sponges

Sample	TTCP (mol)	MCPM (mol)	Hardener	Operability	Consolidation time(min)	Compressive strength (MPa)
1	1	1	0.17M Na_2HPO_4 + 3% citric acid + 0.2% glycerol	√	>30	N/A
2	1.1	1		√	>30	N/A
3	2	1		√	>20	1.09±0.36
4	3.5	1		√	<15	4.39±0.96
5	5	1		√	<5	4.66±1.31
6	10	1		×	N/A	N/A

*Liquid-to-powder ratio=0.36 ml/g

646
647
648

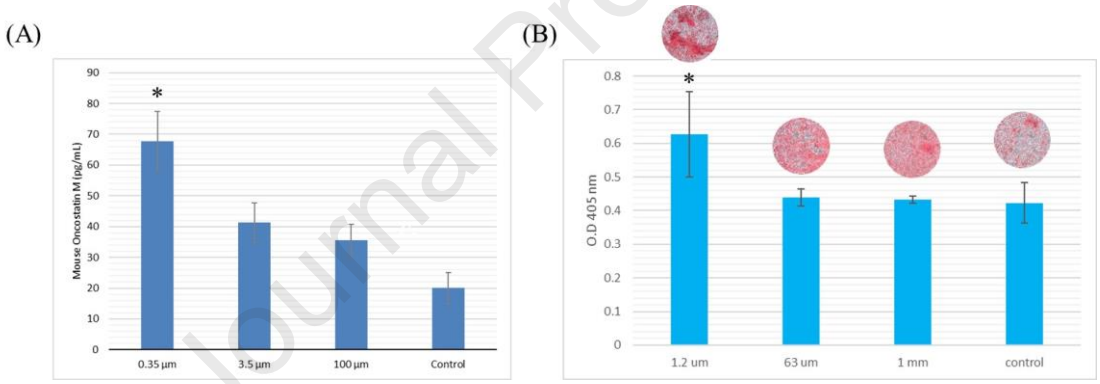

649
650 Appendix 1 (A) Test of mouse oncostatin M (OSM) and (B) Mineralization experiment
651 conducted on different particle sizes of CaP material to validate the advantages of sub-
652 micron particles. (one-way ANOVA, mean ± SD, n=6, *p < 0.05 compared with control).
653